Sensitization of TiO_2 by Phosphonate-Derivatized Proline Assemblies

Scott A. Trammell, John A. Moss, John C. Yang, Bassam M. Nakhle, Cheryl A. Slate, Fabrice Odobel,† Milan Sykora, Bruce W. Erickson,‡ and Thomas J. Meyer*

Department of Chemistry, University of North Carolina at Chapel Hill, CB# 3290, Chapel Hill, North Carolina 27599-3290

Received January 6, 1999

Surface electrochemical and photoelectrochemical measurements on ITO (In_2O_3:Sn) or TiO_2 of two proline assemblies are reported. Surface coverage on ITO of Pbp-pra($Ru^{II}b_2m$)-OH$(PF_6)_2$ and Bpb-pra($Ru^{II}b_2m$)-OCH$_3$$(CF_3CO_2)_2$ are (1.5−2.4) × 10^{-10} mol/cm^2, comparable to monolayer coverages of (1.5−2.5) × 10^{-10} mol/cm^2 for [Ru(bpy)$_2$(4,4′-$(CO_2H)_2$bpy)]$(PF_6)_2$ and [Ru(bpy)$_2$(4,4′-$(PO_3H_2)_2$bpy)]$(Br)_2$. Incident photon-to-current conversion efficiency (IPCE) measured in Gräztel-type photovoltaic cells are sensitive to subtle structural differences in the assemblies. IPCE values for Pbp-pra($Ru^{II}b_2m$)-OH$(PF_6)_2$ and Bpb-pra($Ru^{II}b_2m$)-OCH$_3$$(CF_3CO_2)_2$ are 2% and <0.1%, which are compared to 23% for both [Ru(bpy)$_2$(4,4′-$(PO_3H_2)_2$bpy)]$(Br)_2$ and [Ru(bpy)$_2$(4,4′-$(CO_2H)_2$-bpy)]$(PF_6)_2$ under the same conditions.

Introduction

We have applied the Merrifield solid-phase synthesis technique to the preparation of a family of peptide-based, molecular assemblies containing polypyridyl chromophores. This includes assemblies such as **1** (Chart 1) in which advantage is taken of the tendency of extended oligoprolines to form helical structures. For example, circular dichroism (CD) and ^{1}H NMR studies reveal that **1** is in the proline II form in CH_3CN and H_2O in which the local amide bonds are trans.[1]

We have initiated a systematic study of surface attachment and synthesis of peptide-based assemblies on metal oxide substrates. There is an extensive chemistry of this kind based on carboxylato derivatives where surface binding occurs by H-bonding or ester formation or a combination of the two.[2−7] Notable in this regard is the visible sensitization of TiO_2 by adsorbed polypyridyl complexes of Ru(II) which has provided the basis for a family of solution-based, photovoltaic devices.[7−11]

A disadvantage of carboxylic binding to these surfaces is the fragility of the resulting surface link toward hydrolysis. Recent reports suggest that much higher surface stabilities can be achieved by utilization of phosphonic acid derivatives and phosphonate-surface binding.[12−14]

We report here the properties, metal oxide surface binding, and visible TiO_2 sensitization of the bis(phosphonate) complex, **2**, and proline-derivatized assemblies **3** and **4** (Chart 2). Assemblies **3** and **4** feature the key elements required for surface construction of higher order, more complex assemblies—a phosphonic acid group for surface binding, a Ru−bpy chromophore, and a free acid or ester group on a proline unit for building higher assemblies.

Experimental Section

Materials. The solvents CH_3CN (Baxter; B&J, high purity), ethanol (EtOH) (AAPER Alcohol and Chemical Co, absolute) and propylene carbonate (Sigma-Aldrich) were used as received. Solvents for the preparation of metal complexes were dried before use by standard methods. [N(n-C_4H_9)$_4$](PF_6) (TBAH) was purchased from Sigma Aldrich and recrystallized twice from ethanol. Tin-doped indium oxide (ITO, In_2O_3:Sn) coated glass slides were purchased from Delta Tech. Ltd., Stillwater, MN. Column chromatography was performed on silica gel: Kieselgel 60, 230−400 mesh, Merck 9385. Procedures for the preparations of 4,4′-$(PO_3Et_2)_2$bpy,[15] Ru(bpy)$_2Cl_2$,[16] [Ru(bpy)$_2$(4,4′-$(CO_2H)_2$bpy)]$(PF_6)_2$,[6] Pbp-pra($Ru^{II}b_2m$)-OH$(PF_6)_2$,[17] and Bpb-pra-($Ru^{II}b_2m$)-OCH$_3$$(CF_3CO_2)_2$[18] were reported previously.

Synthesis. [Ru(bpy)$_2$(4,4′-$(PO_3Et_2)_2$bpy)]$(PF_6)_2$. A solution of 213 mg of 4,4′-$(PO_3Et_2)_2$bpy (0.50 mmol) and 310 mg of Ru(bpy)$_2Cl_2$·$2H_2O$ (0.60 mmol) in 50 mL of 9/1 EtOH/H_2O was heated to reflux under

† Present address: Laboratoire de Synthese Organique, Faculte des Sciences et des Techniques de Nantes, Nantes, France.

‡ Deceased.

(1) McCafferty, D. G.; Friesen, D. A.; Danielson, E.; Wall, C. G.; Saderholm, M. J.; Erickson, B. W.; Meyer, T. J. *Proc. Natl. Acad. Sci. U.S.A.* **1996**, *93*, 8200.
(2) Argazzi, R.; Bignozzi, C. A.; Heimer, T. A.; Castellano, F. N.; Meyer, G. J. *Inorg. Chem.* **1994**, *33*, 5741−5749.
(3) Amadelli, R.; Argazzi, R.; Bignozzi, C. A.; Scandola, F. *J. Am. Chem. Soc.* **1990**, *112*, 7099−7103.
(4) Dabestani, R.; Bard, A. J.; Campion, A.; Fox, M. A.; Mallouk, T. E.; Webber, S. E.; White, J. M. *J. Phys. Chem.* **1988**, *92*, 1872−1878.
(5) Vlachopoulos, N.; Liska, P.; Augustynski, J.; Grätzel, M. *J. Am. Chem. Soc.* **1988**, *110*, 1216−1220.
(6) Meyer, T. J.; Meyer, G. J.; Pfennig, B. W.; Schoonover, J. R.; Timpson, C. J.; Wall, J. F.; Kobusch, C.; Chen, X.; Peek, B. M.; Wall, C. G.; Ou, W.; Erickson, B. W.; Bignozzi, C. A. *Inorg. Chem.* **1994**, *33*, 3952−3964.
(7) O'Regan, B.; Moser, J.; Anderson, M.; Grätzel, M. *J. Phys. Chem.* **1990**, *94*, 8720−8726.
(8) Meyer, G. J. *J. Chem. Educ.* **1997**, *74*, 652−656.
(9) Nazeeruddin, M. K.; Kay, A.; Rodicio, I.; Humphry-Baker, R.; Muller, E.; Liska, P.; Vlachopoulos, N.; Grätzel, M. *J. Am. Chem. Soc.* **1993**, *115*, 6382−6390.
(10) Heimer, T. A.; D'Arcangelis, S. T.; Farzad, F.; Stipkala, J. M.; Meyer, G. J. *Inorg. Chem.* **1996**, *35*, 5319−5324.
(11) O'Regan, B.; Grätzel, M. *Nature* **1991**, *353*, 737−740.
(12) Péchy, P.; Rotzinger, F. P.; Nazeeruddin, M. K.; Kohle, O.; Zakeeruddin, S. M.; Humphry-Baker, R.; Grätzel, M. *Chem. Commun.* **1995**, 65−66.
(13) Hupp, J. T.; Yan, S. G. *J. Phys. Chem.* **1996**, *100*, 6867.
(14) Trammell, S. A.; Wimbish, J. C.; Odobel, F.; Gallagher, L. A.; Narula, P. M.; Meyer, T. J. *J. Am. Chem. Soc.* **1998**, *120*, 13248−13249.
(15) Penicaud, V.; Ododel, F.; Bujoli, B. *Tetrahedron Lett.* **1998**, *39*, 3689.
(16) Meyer, T. J.; Salmon, D. J.; Sullivan, B. P. *Inorg. Chem.* **1978**, *17*, 3334−3337.
(17) Slate, C. A., Ph.D. Dissertation, The University of North Carolina, Chapel Hill, NC, 1997.
(18) Nakhle, B. M.; Trammell, S. A.; Sigel, K. M.; Meyer, T. J.; Erickson, B. W. *Tetrahedron* **1999**, *55*, 2835−2846.

10.1021/ic990052t CCC: $18.00
Published on Web 07/16/1999

Chart 1

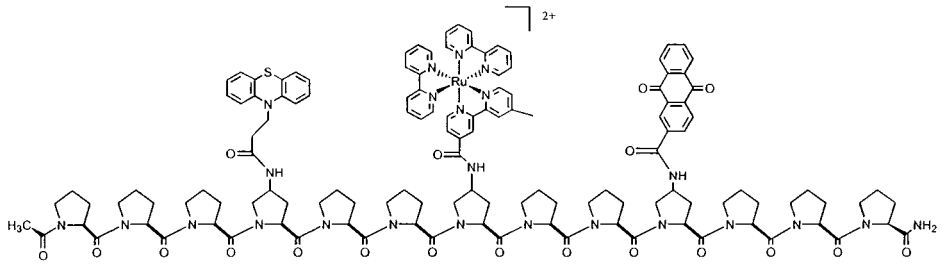

1

Chart 2

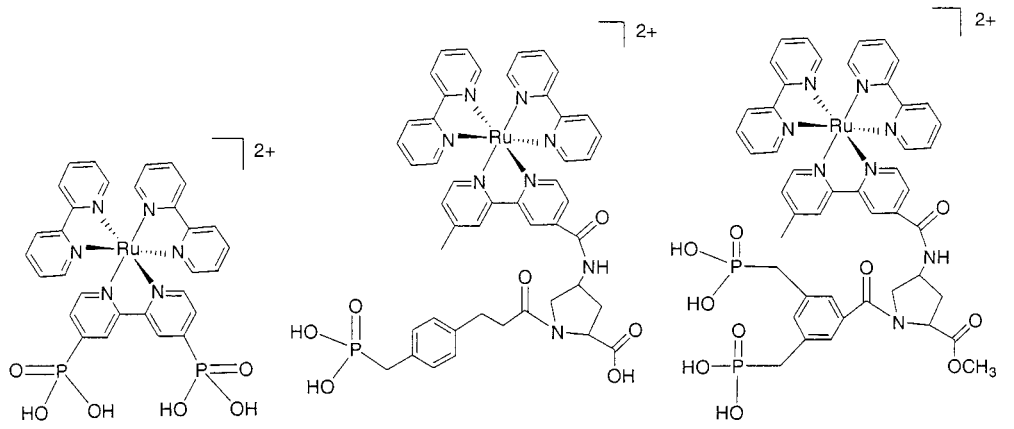

[Ru(bpy)$_2$(4,4′-(PO$_3$H$_2$)$_2$bpy)](Br)$_2$ **2** Pbp-pra(Ru^{II}b$_2$m)-OH(PF$_6$)$_2$ **3** Bpb-pra(Ru^{II}b$_2$m)-OCH$_3$(CF$_3$CO$_2$)$_2$ **4**

argon for 3 h. During heating, the reaction flask was covered with aluminum foil to protect it from ambient light. The solvent was removed by rotary evaporation. The crude deep red residue was dissolved in a minimum amount of an acetone/water (9/1) mixture and loaded on a silica column for chromatography. Elution with acetone/water (8/2) eliminated the unreacted Ru(bpy)$_2$Cl$_2$. An acetone/water/aqueous saturated KNO$_3$ (80 mL/20 mL/10 drops) mixture afforded the desired complex [Ru(bpy)$_2$(4,4′-(PO$_3$Et$_2$)$_2$bpy)](NO$_3$)$_2$. The pure fractions were gathered after the acetone was rotary evaporated. A 0.3 g amount of KPF$_6$ was added to the resulting aqueous solution and was washed 2 times with CH$_2$Cl$_2$ to extract complex as a PF$_6^-$ salt. The organic phase was dried over MgSO$_4$ and the solvent removed yielding 390 mg of complex. ^{1}H NMR (400 MHz, CD$_3$CN, δ): 1.32 (m, 12H, CH$_3$); 4.20 (m, 8H, CH$_2$); 7.45 (m, 4H, H5a, H5′a); 7.64 (m, 2H, H5, H5′); 7.72-(m, 4H, H6a, H6′a); 7.95 (m, 4H, H6, H6′), 8.10 (m, 4H, H4a, H4′a); 8.54(d, 4H, H3a,H3′a); 8.80 (d, 2H, H3,H3′). ^{31}P NMR (200 MHz, CD$_3$CN, δ): 10.32. FAB-MS (*m*/*e*): calcd for C$_{38}$H$_{42}$N$_6$RuP$_2$, 842; found, 842.

[Ru(bpy)$_2$(4,4′-(PO$_3$H$_2$)$_2$bpy)](Br)$_2$ (2). A 400 mg (0.35 mmol) amount of [Ru(bpy)$_2$(4,4′-(PO$_3$Et$_2$)$_2$bpy)](PF$_6$)$_2$ was dissolved in 20 mL of dry DMF, 0.6 mL (4.5 mmol) of Me$_3$SiBr was added, and the mixture was heated at 60 °C under argon and shielded from light for 18 h. DMF and excess Me$_3$SiBr were eliminated under vacuum with a liquid-N$_2$ trap. The solid residue was dissolved in MeOH and stirred at room temperature for 3 h. To the deep orange solution was added diethyl ether until precipitation occurred, and the red solid was filtered out and washed with diethyl ether. Drying under the vacuum pump afforded 300 mg of pure [Ru(bpy)$_2$(4,4′-(PO$_3$H$_2$)$_2$bpy)](Br)$_2$. ^{1}H NMR (400 MHz, CD$_3$CN, δ): 7.51 (m, 4H, H5a, H5′a); 7.75 (m, 2H, H5, H5′), 7.82(m, 4H, H6a, H6′a); 8.01 (m, 2H, H6, H6′); 8.15 (t, 4H, H4a, H4′a), 8.73-(d, 4H, H3a,H3′a); 8.91 (d, 2H, H3,H3′). ^{31}P NMR (200 MHz, CD$_3$-OD, δ): 6.06. UV−vis [CH$_3$CN; λ_{max}, nm (ϵ, M^{-1} cm^{-1})]: 458 (11 600).

Procedures. Electrode Preparation. ITO. Before surface attachment, ITO electrodes were washed in a 5:1:1 solution of H$_2$O, H$_2$O$_2$, and NH$_4$OH and thoroughly rinsed with purified water. These electrodes were heated to 400 °C for 5 min over O$_2$. After the electrodes cooled, they were placed in solutions 1×10^{-4} M in metal complex as their respective salts in CH$_3$CN for 16−72 h.

TiO$_2$ and ZrO$_2$. Nanocrystalline TiO$_2$ (or ZrO$_2$) films on ITO electrodes and TiO$_2$ (or ZrO$_2$) colloids were prepared by a previously published method.[10] A portion of the ITO surface was masked with Scotch tape, and the TiO$_2$ (or ZrO$_2$) colloid was spread with a glass rod. The resulting films were allowed to dry for 30 min, and the electrodes were cut into ∼9 mm wide pieces. They were heated to 400 °C for 30 min over O$_2$, cooled, and placed in solutions 2×10^{-4} M in metal complex as their respective salts in EtOH for 16 h. The peptides Pbp-pra(Ru^{II}b$_2$m)-OH^{2+} and Bpb-pra(Ru^{II}b$_2$m)-OCH$_3^{2+}$ were deposited by soaking their PF$_6^-$ or CF$_3$CO$_2^-$ salts for 48−72 h in ethanolic solutions 0.01 mM in peptide. After derivatization, the electrodes were rinsed with ethanol and stored in a fresh ethanol solution until use.

Measurements. Cyclic voltammetric experiments were conducted with a PAR 273 potentiostat by using the standard three-electrode configuration in a one compartment cell. The medium was 0.1 M [N(*n*-C$_4$H$_9$)$_4$](PF$_6$) (TBAH) in CH$_3$CN. The reference electrode was Ag/AgNO$_3$ (0.1 M TBAH and 0.01 M AgNO$_3$ in CH$_3$CN) which was 300 mV more positive than SCE. The counter electrode and working electrodes were Pt. For surface measurements, cyclic voltammetric experiments were conducted by using the standard three-electrode configuration in a three-compartment cell. The reference electrodes were SSCE in the case of water as solvent or Ag/AgNO$_3$ with CH$_3$CN as solvent. The counter electrode was Pt, and the working electrode was the derivatized ITO. Surface coverage of electroactive complex was calculated from cyclic voltammograms. Areas under voltammetric waves were integrated after correction for background current and divided by scan rate and electron charge by using an in-house program. Electrode areas were between 2 and 3 cm^2 and used without correction for surface roughness.

UV−visible measurements were made with a HP-8452 diode array spectrometer and referenced against a solvent blank. The TiO$_2$ electrodes were placed in a 1 cm cuvette containing CH$_3$CN and positioned against the side of the cell for each measurement. Surface coverages of metal complexes, Γ in mol/cm^2, were calculated from absorbance measurements after subtraction of a blank TiO$_2$ electrode. Surface coverage of

Table 1. Photophysical and Electrochemical Properties of the Sensitizers in CH_3CN at 25 °C

complex[a]	$E_{1/2}(Ru^{III/II})$ (V)	λ_{abs}[c] (nm)	λ_{em}[c] (nm)	$\sim E_{1/2}(Ru^{III/II*})$[d]
$Ru^{II}(bpy)_2(4,4'\text{-}(PO_3H_2)_2bpy)^{2+}$ (**2**)	1.39	456	642	−0.70
$Pbp\text{-}pra(Ru^{II}b_2m)\text{-}OH^{2+}$ (**3**)	1.29	458	646	−0.79
$Bpb\text{-}pra(Ru^{II}b_2m)\text{-}OCH_3^{2+}$ (**4**)	1.29	458	646	−0.79
$Ru^{II}(bpy)_2(4,4'\text{-}(CO_2H)_2bpy)^{2+}$ (**5**)	1.38[e]	474	680	−0.60

[a] **2** as a Br^- salt, **4** as a ClO_4^- salt, and **3** and **5** as PF_6^- salts. [b] Measured at a Pt working electrode vs SCE in CH_3CN 0.1 M in TBAH. [c] MLCT absorption and emission maxima. [d] Excited-state reduction potentials estimated from $E_{1/2}(Ru^{III/II*}) = E_{1/2}(Ru^{III/II}) - (E_o(\text{in cm}^{-1})/8066 + \chi_o \text{ (in eV)})$, $E_o \geq E_{1/2}$ and $\chi_o \approx 0.1$. [e] From ref 6.

the geometric areas of the electrodes were calculated from the relationship $A(\lambda) = 1000\Gamma\epsilon(\lambda)$. $A(\lambda)$ and $\epsilon(\lambda)$ are the absorbance and molar extinction coefficient in M^{-1} cm^{-1} with the latter taken as the value in CH_3CN; $\lambda_{max} = 452$ nm (13 000 M^{-1} cm^{-1}) for $[Ru(bpy)_2(4,4'\text{-}(CO_2H)_2bpy)](PF_6)_2$. For $Pbp\text{-}pra(Ru^{II}b_2m)\text{-}OH(PF_6)_2$ and $Bpb\text{-}pra(Ru^{II}b_2m)\text{-}OCH_3(CF_3CO_2)_2$ the molar extinction coefficient for the model complex $Ru(bpy)_2(4\text{-}CH_3\text{-}4'\text{-}CONHBzbpy)(PF_6)$ was used; $\lambda_{max} = 458$ nm (14 600 M^{-1} cm^{-1}).[19]

Photoelectrochemistry. Photocurrent measurements were carried out in a thin-layer, two-electrode cell. The counter electrode was a Pt foil sealed in a block of epoxide resin (Buehler) to form the cell base. The TiO_2 electrode was sandwiched against the counter electrode with a 0.1 mm Teflon spacer, and a propylene carbonate solution 0.5 M in NaI and 0.05 M in I_2 was drawn into the cell by capillary action. The irradiation source was a 75 W xenon lamp powered by a high precision constant current source coupled to a f4 matched monochromator with 1200 lines/in. gratings. The light from the monochromator was passed through two glass lenses and onto either the IL 500 radiometer for light intensity measurement or the thin-layer TiO_2 photoelectrochemical cell for photocurrent measurements. Incident photon-to-current conversion efficiencies (IPCE) at each incident wavelength were calculated from the equation

$$\text{IPCE}(\lambda) = \frac{(1240 \text{ eV·nm})I_{ph}}{\lambda P_0} \quad (1)$$

In this equation, I_{ph} is the incident photocurrent density in mA cm^{-2}, λ is the wavelength of incident radiation in nm, and P_0 is photon flux in mW cm^{-2}. The absorbed photon to current conversion efficiency (APCE) was calculated from the light-harvesting efficiency (LHE, the percentage of light absorbed by the adsorbed chromophore defined as $\text{LHE} = 1 - 10^{-A(\lambda)}$ with $A(\lambda)$ the absorbance at λ) using eq 2.

$$\text{APCE} = \text{IPCE/LHE} \quad (2)$$

Emission Spectroscopy. Room-temperature, CW emission spectra were recorded on a Spex Fluorolog-F212 emission spectrometer equipped with a 450-W xenon lamp and a cooled R928 photomultiplier tube. For surface measurements, the electrodes were placed in standard cuvette with propylene carbonate in the external solution. Emission was collected at a 90° angle from the excitation source with the electrode at 45° to the excitation beam. The emission was corrected for the spectral sensitivity of the detector.

Emission lifetimes were measured following laser flash excitation at 455 nm by using a PRA nitrogen laser model LN1000 and a PRA dye laser model LN102. Emission decays were monitored at 640 nm by using an PRA monochromator model B204-3 and a Hamamatsu R-928 phototube and recorded on a LeCroy 7200A digital oscilloscope interfaced to an IBM-PC. Intensity−time decay profiles were fit to the biexponential function in eq 3. The average lifetime was calculated by using eq 4.

$$I(t) = a \exp\left(-\frac{t}{\tau_1}\right) + (1-a)\exp\left(-\frac{t}{\tau_2}\right) \quad (3)$$

$$\langle\tau\rangle = a\tau_1 + (1-a)\tau_2 \quad (4)$$

Results

In CH_3CN 0.1 M in TBAH, $E_{1/2} = 1.36$ V vs SCE for the $Ru^{III/II}$ couple of **2**, and, on ITO deposited from CH_3CN, $E_{1/2} =$ 1.39 V. Surface cyclic voltammograms were stable to repetitive cycling through the $Ru^{III/II}$ couple for extended periods. Integration of current−potential waveforms gave a limiting surface coverage of 2.5×10^{-10} mol/cm^2. Peptide complexes **3** and **4** display reversible $Ru^{III/II}$ couples at 1.29 V. **3** forms an electroactive monolayer with $\Gamma = 2.6 \times 10^{-10}$ mol/cm^2 when deposited from CH_3CN, and **4** a coverage of 1.8×10^{-10} mol/cm^2. Successive cycling (>100) through the $Ru^{III/II}$ surface couples of **3** reveals a slowly evolving, irreversible electrochemistry with a new couple growing in at 0.80 V vs SCE.

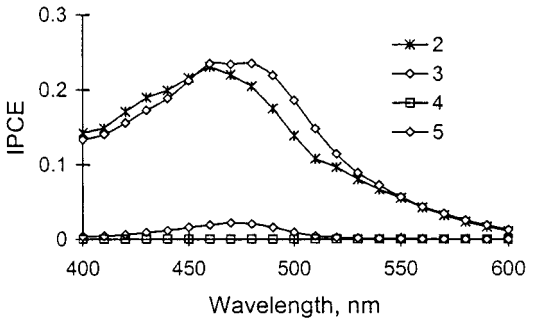

Figure 1. Photocurrent action spectra on TiO_2:$Ru^{II}(bpy)_2(4,4'\text{-}(PO_3H_2)_2\text{-}bpy^{2+}$ (**2**), $Pbp\text{-}pra(Ru^{II}b_2m)\text{-}OH^{2+}$ (**3**), $Bpb\text{-}pra(Ru^{II}b_2m)\text{-}OCH_32+$ (**4**), and $Ru^{II}(bpy)_2(4,4'\text{-}(CO_2H)_2bpy^{2+}$ (**5**). Spectra were measured in propylene carbonate 0.5 M in NaI and 0.05 M in I_2 in a thin-layer, two-electrode cell as described in the Experimental Section.

The respective salts of **2**−**4** adsorb onto TiO_2 from EtOH as shown by UV−visible measurements in the $Ru^{II} \rightarrow$ bpy metal-to-ligand charge transfer (MLCT) region from 350 to 820 nm. For peptide complexes **3** and **4**, surface coverages on TiO_2 (mol/cm^2) estimated by absorbance measurement are less than for **2** and $[Ru(bpy)_2(4,4'\text{-}(CO_2H)_2)bpy]^{2+}$(**5**) (Table 1).

Phosphonate binding imparts considerable stability in water. At pH 1 only ~10% loss in coverage occurs over a period of several days for all three of the phosphonate complexes. At pH > 3, **3** and **4** desorb on a time scale of minutes. **2** is stable for several weeks in water at pH = 7.

Figure 1 shows plots of incident photon-to-current efficiency (IPCE) vs excitation wavelength for the three phosphonate-derivatized sensitizers. These results are reported relative to **5**. When adsorbed to TiO_2, **5** and **2** have similar IPCE's of about 23% under our experimental conditions. No effort was made to maximize the IPCE values. These results show that the IPCE value for **3** (~ 2%) is ~10× lower than for **2** and that the IPCE value for **4** is <0.1%.

Lifetime and emission data for **3** and **4** on TiO_2 are given in Table 3, and relative emission intensities of **4** and **2** on TiO_2 in propylene carbonate 0.1 M in $NaClO_4$ are compared in Figure 2. Average surface quenching rate constants, $\langle k\rangle$, were calculated from the difference in average lifetimes on ZrO_2 and TiO_2 by using eq 5. In this treatment, which is only approximate, the

$$\langle k\rangle = \frac{1}{\langle\tau_{TiO_2}\rangle} - \frac{1}{\langle\tau_{ZrO_2}\rangle} \quad (5)$$

(19) Dupray, L. M.; Meyer, T. J. *Inorg. Chem.* **1996**, *35*, 6299−6307.

Table 2. Photoelectrochemical and Electrochemical Properties on Oxide Surfaces with CH_3CN in the External Solution at 25 °C

complex	$E_{1/2}(Ru^{III/II})^a$ (V)	$10^{10}\Gamma$(ITO) (mol/cm^2)	$\Gamma(TiO_2)$ (mol/cm^2)	LHE_{max}	$IPCE_{max}{}^b$	$APCE_{max}{}^c$
$Ru^{II}(bpy)_2(4,4'\text{-}(PO_3H_2)_2bpy)^{2+}$ (**2**)	1.36	2.5	1.7×10^{-7}	0.99	0.23 ± 0.05	0.23
Pbp-pra($Ru^{II}b_2$m)-OH^{2+} (**3**)	1.28	2.6	7.2×10^{-8}	0.90	0.02 ± 0.01	0.022
Bpb-pra($Ru^{II}b_2$m)-$OCH_3{}^{2+}$ (**4**)	1.30	1.8	4.6×10^{-8}	0.80	<0.001	<0.001
$Ru^{II}(bpy)_2(4,4'\text{-}(CO_2H)_2bpy)^{2+}$ (**5**)	1.34	1.5	1.3×10^{-7}	0.98	0.23 ± 0.05	0.23

[a] On ITO in CH_3CN 0.1 M in TBAH vs SCE. [b] IPCE (average of 3−4 electrodes) measured in propylene carbonate 0.5 M in NaI and 0.05 M in I_2. [c] Calculated from eq 2.

Table 3. Photophysical Parameters on Oxides in Propylene Carbonate 0.1 M in $NaClO_4$, Ar Purged[a]

		TiO_2				ZrO_2				
complex	λ_{em} (nm)	a	τ_1 (ns)	τ_2 (ns)	$\langle\tau\rangle$ (ns)	a	τ_1 (ns)	τ_2 (ns)	$\langle\tau\rangle$ (ns)	$\langle k\rangle$ (s^{-1})
$Ru^{II}(bpy)_2(4,4'\text{-}(PO_3H_2)_2bpy^{2+}$ (**2**)	654	0.83	15	87	27	0.50	94	497	297	$>3.3 \times 10^7$
Pbp-pra($Ru^{II}b_2$m)-OH^{2+} (**3**)	664	0.60	86	432	224	0.51	89	467	274	8.1×10^5
Bpb-pra($Ru^{II}b_2$m)-$OCH_3{}^{2+}$ (**4**)	664	0.42	136	749	490	0.47	175	867	541	1.9×10^5

[a] Kinetic decay parameters from fits of emission decays to eq 3. $\langle\tau\rangle$ calculated from eq 4. [b] $\langle k\rangle = 1/\langle\tau_{TiO_2}\rangle - 1/\langle\tau_{ZrO_2}\rangle$.

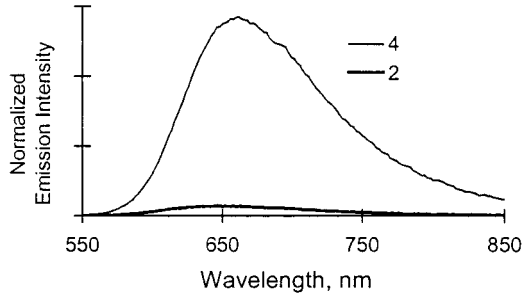

Figure 2. Emission intensity of $Ru^{II}(bpy)_2(4,4'\text{-}(PO_3H_2)_2bpy^{2+}$ (**2**) and Bpb-pra($Ru^{II}b_2$m)-$OCH_3{}^{2+}$ (**4**) adsorbed to TiO_2 measured in propylene carbonate 0.1 M in $NaClO_4$, air-saturated. Emission intensities were normalized for film absorbance at the excitation wavelength of 460 nm.

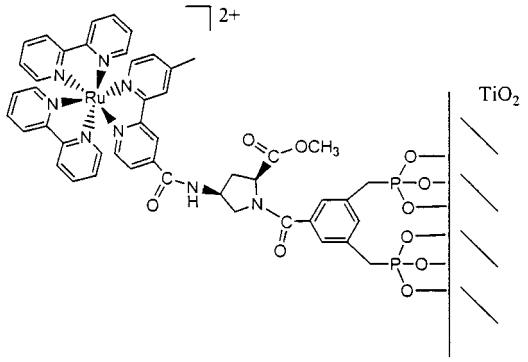

Figure 3. Extended structure for Bpb-pra($Ru^{II}b_2$m)-$OCH_3{}^{2+}$ (**4**) on TiO_2.

surface environments of ZrO_2, on which quenching does not occur, is assumed to be comparable to that of TiO_2. Results are listed in Table 3. The lifetime of the MLCT excited state of **2** was too short to resolve on our apparatus. Consistent with earlier studies,[2] there is a small amount of residual emission most likely from Ru complexes on TiO_2 that do not photoinject efficiently. Recent reports have shown that the MLCT excited states of **5** and related complexes are quenched by electron transfer on TiO_2 on the femtosecond time scale.[20−22]

Discussion

The synthesis of the phosphonate-containing proline assemblies has been described in detail elsewhere.[17,18] Incorporation of the phosphonic acid groups creates a basis for stable surface adsorption, and the surface linkage strategy is a success. Stability studies on TiO_2 reveal that surface structures prepared by simple soaking are stable for extended periods in CH_3CN or EtOH and for several days in water at pH 1.

Electrochemical studies of both **3** and **4** on ITO reveal the existence of the expected surface-bound $Ru^{III/II}$ couples, at 1.29 V vs SCE. The experimental surface coverages of $\Gamma = (1.5-2.6) \times 10^{-10}$ mol/cm^2 are in the same range as for modified surfaces formed from **2** or from carboxylic acid derivatives such as **5**. Given the ∼14 Å diameters of the metal complexes, a monolayer coverage of 1.1×10^{-10} mol/cm^2 is consistent with close-packed surface structures assuming a relatively flat surface.[6] This is consistent with extended structures, such as the one illustrated in Figure 3 which features phosphonate binding to the surface and hydrocarbon chains extended off the electrode surface. The higher coverage of 2.6×10^{-10} mol/cm^2 provides evidence that the ITO surface is slightly rough.

The electrochemical properties of **3** are complicated by a slow chemical change that occurs upon repeated cycling to Ru(III). It is accompanied by a change in $E_{1/2}$ for the Ru(III/II) couple from 1.29 to 0.80 V vs SCE which is comparable, for example, with the difference in $E_{1/2}$ values between $[Ru(bpy)_3]^{2+}$ (1.29 V vs SCE) and *cis*-$[Ru(bpy)_2(py)Cl]^+$ (0.79 V),[23] suggesting replacement of a single arm of one of the bpy ligands perhaps by the free carboxylato group. We have been unable to elucidate the nature of the product in further detail.

The IPCE data show that photoinjection from **2** adsorbed on TiO_2 is efficient, comparable to that from the dicarboxylic acid derivative **5**. In this case there is direct bpy-phosphonate bonding to the surface and the phosphonate ester or acid ligand has the lower-lying π^* level. It also provides an orbital basis for direct electronic coupling with the surface.

There is no basis for direct electronic coupling for **3** or **4,** and their IPCE values are greatly reduced. Comparison of lifetime data on ZrO_2 and TiO_2 shows that the fraction of quenching on TiO_2 is 18.2% for **3** and 9.4% for **4**. Fractional IPCE values normalized to **2** are 8.7% for **3** and 0.4% for **4**.

These comparisons suggest that small structural differences in the linkage chemistry can result in considerable changes in injection yield. Both surface quenching and IPCE are enhanced

(20) Hannappel, T.; Burfeindt, B.; Storck, W.; Willig, F. *J. Phys. Chem. B* **1997**, *101*, 6799−6802.
(21) Rehm, J. M.; McLendon, G. L.; Nagasawa, Y.; Yoshihara, K.; Moser, J.; Gratzel, M. *J. Phys. Chem.* **1996**, *100*, 9577−9578.
(22) Moser, J.-E.; Gratzel, M.; Durrant, J. R.; Klug, D. R. *Femtosecond Interfacial Electron Transfer in The Dye-Sensitization of a Wide Band gap Semiconductor*; Moser, J.-E., Gratzel, M., Durrant, J. R., Klug, D. R., Eds.; World Scientific: London, 1996; pp 495−498.
(23) Sullivan, B. P.; Conrad, D.; Meyer, T. J. *Inorg. Chem.* **1985**, *24*, 3640.

for **3** compared to **4**. Although surface coverages are comparable, there may be a role, at least in part, for both phosphonate and carboxylate surface binding, based on the structure of **3**. This would decrease the distance between the excited state and the TiO_2 surface. In **4** the carboxylate group on the proline is ester-protected. In fully extended structures, the distance of the Ru−bpy chromophore from the surface could be as large as ∼16 Å for **3** and ∼14 Å for **4**.[24] Similarly, low IPCE's have been reported for Ru−bpy chromophores covalently linked to TiO_2 by the silane linking agent *N*-(2-aminoethyl)-(3-aminopropyl)methyldimethoxysilane.[4] It is also known that direct binding to TiO_2 is not a requirement for efficient photoinjection. Bignozzi and Meyer have demonstrated that efficient photoinjection occurs following excitation of the remote Ru−bpy chromophore in the CN-bridged assembly $[(bpy)_2Ru(NC)Re(CO)_3(4,4'\text{-}(CO_2H)_2bpy)](PF_6)$.[25]

The fact that there is experimentally insignificant photoinjection by **4** is also an important observation. It points to the possibility of preparing interfacial molecular structures in which excitation and electron transfer can occur free of electron-transfer quenching by the electrode. By incorporating the chromophore-quencher apparatus of assemblies such as **1**, it may be possible to achieve molecular-level photoinduced redox separation with the electrode used solely as a collector. An additional topic that we hope to explore with surface-bound polyproline assemblies is the distance dependence of surface quenching.

The results described here point to the viability of metal oxide surface modification by phosphonate binding of proline assemblies. Experiments are currently being undertaken to investigate whether the unbound carboxylic group can be derivatized by amide coupling thus providing a synthetic basis for constructing complex peptide assemblies directly on the electrode surface.

Acknowledgments for the support of the work are made to the Army Research Office under Grant No. DAAH04-95-1-0144 and to the NSF for Grant No. CHE-9705724.

IC990052T

(24) Modeled by using CS Chem3D Pro, version 4.0, CambridgeSoft Corp., Cambridge, MA, 1997.

(25) Argazzi, R.; Bignozzi, C.; Heimer, T. A.; Meyer, G. J. *Inorg. Chem.* **1997**, *36*, 2−3.